Translational Oncology
www.transonc.com

Volume 12 Number 1 January 2019 pp. 96–105 96

Targeting DDX3 in Medulloblastoma Using the Small Molecule Inhibitor RK-33

Saritha Tantravedi[*], Farhad Vesuna[*], Paul T. Winnard Jr.[*], Allison Martin[†], Michael Lim[‡], Charles G. Eberhart[§], Cynthia Berlinicke[¶], Eric Raabe[#], Paul J. van Diest[†,] and Venu Raman[*,†,**]**

[*]Division of Cancer Imaging Research, Department of Radiology and Radiology Science, Johns Hopkins University, School of Medicine, Baltimore, MD; [†]Department of Oncology, Johns Hopkins University, School of Medicine, Baltimore, MD; [‡]Department of Neurosurgery, Johns Hopkins Hospital, Baltimore, MD; [§]Department of Pathology and Oncology, Johns Hopkins Hospital, Baltimore, MD; [¶]Wilmer Eye Institute, Johns Hopkins University, School of Medicine, MD; [#]Department of Pediatric Oncology and Pathology, Johns Hopkins Hospital, Baltimore, MD; [**]Department of Pathology, University Medical Center Utrecht, Utrecht, The Netherlands

Abstract

Medulloblastoma is the most common malignant tumor that arises from the cerebellum of the central nervous system. Clinically, medulloblastomas are treated by surgery, radiation, and chemotherapy, all of which result in toxicity and morbidity. Recent reports have identified that DDX3, a member of the RNA helicase family, is mutated in medulloblastoma. In this study, we demonstrate the role of DDX3 in driving medulloblastoma. With the use of a small molecule inhibitor of DDX3, RK-33, we could inhibit growth and promote cell death in two medulloblastoma cell lines, DAOY and UW228, with IC50 values of 2.5 μM and 3.5 μM, respectively. Treatment of DAOY and UW228 cells with RK-33 caused a G1 arrest, resulted in reduced TCF reporter activity, and reduced mRNA expression levels of downstream target genes of the WNT pathway, such as Axin2, CCND1, MYC, and Survivin. In addition, treatment of DAOY and UW228 cells with a combination of RK-33 and radiation exhibited a synergistic effect. Importantly, the combination of RK-33 and 5 Gy radiation caused tumor regression in a mouse xenograft model of medulloblastoma. Using immunohistochemistry, we observed DDX3 expression in both pediatric (55%) and adult (66%) medulloblastoma patients. Based on these results, we conclude that RK-33 is a promising radiosensitizing agent that inhibits DDX3 activity and down-regulates WNT/β-catenin signaling and could be used as a frontline therapeutic strategy for DDX3-expressing medulloblastomas in combination with radiation.

Translational Oncology (2019) 12, 96–105

Introduction

Medulloblastoma is the most common malignant form of pediatric brain tumor that occurs in the cerebellum of the central nervous system [1]. Despite treatment advances in recent years, current treatment strategies are associated with long-term toxicities. About 40% of patients experience recurrence of the disease and 30% of patients will eventually die [2]. Current standard treatments include surgical resection and craniospinal irradiation, followed by chemotherapy. Although these strategies have the potential to increase the

Address all correspondence to: Venu Raman, Division of Cancer Imaging Research, Russell H. Morgan Department of Radiology and Radiological Science, Johns Hopkins University School of Medicine, 720 Rutland Avenue, Traylor 340, Baltimore, MD 21205.
E-mail: vraman2@jhmi.edu
Received 9 July 2018; Revised 31 August 2018; Accepted 7 September 2018

1936-5233/19
https://doi.org/10.1016/j.tranon.2018.09.002

survival of 70–80% of patients with medulloblastoma, they are associated with serious treatment-induced morbidity. Histologically, medulloblastoma is defined into four subtypes: classic, desmoplastic/nodular; medulloblastoma with extensive nodularity; and large cell/anaplastic [3]. Genetically, medulloblastoma is subtyped into five subgroups: WNT-activated; Sonic hedgehog (SHH)-activated and p53-mutant; SHH-activated and p53-wildtype; non-WNT/non-SHH Group 3; and non-WNT/non-SHH Group 4 [4]. More recently, medulloblastoma has been subtyped into 7 distinct groups [5,6]. Approximately 10% of medulloblastoma show up-regulation of the WNT pathway with mutations mainly in β-catenin (*CTNNB1*), which is the principal effector of the WNT pathway [7–10]. Less common mutations, including adenomatous polyposis coli (APC), Axin1, and Axin2, which are the key factors in the WNT signaling pathway, are also found in medulloblastoma [7,11]. Somatic mutations in Smoothened (SMO), Suppressor of Fused (SUFU), and Patched-1 (PTCH-1) are the molecular abnormalities found in SHH-type medulloblastoma [12–14]. Group 3 and group 4 tumors are associated with genomic instability [11] and MYC amplification [15,16].

DDX3, an RNA helicase, is involved in many biological activities that regulate multiple steps in gene expression, such as transcription [17,18], mRNA translation [18,19], splicing [20], and nuclear export [21,22]. However, mutations in DDX3 have been reported in various cancers, such as chronic lymphocytic leukemia [23], head and neck squamous cell carcinomas [24], and T-cell acute lymphoblastic leukemia [25]. About 8% of medulloblastoma cases involve mutations in DDX3, of which 11% involve the pediatric WNT- and -SHH subtypes [26]. Mutations in DDX3 lead to the activation of mutated β-catenin in TCF/LEF reporter assays, suggesting the oncogenic role of DDX3 in medulloblastoma [27]. DDX3 is also involved in the potentiation of β-catenin signaling through translational regulation of Rac1 in a helicase-dependent manner [28]. In colorectal cancer, DDX3, acting as a mediator in the activation of β-catenin through the CK1ε/Dvl2 axis, is associated with tumor invasion and a worse prognosis [29]. In recent studies, we have shown that RK-33 impaired WNT signaling through the disruption of the DDX3-β-catenin pathway in both lung [30] and colorectal cancers [31]. We have also shown that RK-33, in combination with radiation, induced tumor regression in mouse models of lung cancer [30]. Moreover, RK-33 specifically promoted radiation sensitization in DDX3 over-expressing cells [30,32].

To validate the functional utility of inhibiting DDX3 activity for tumor ablation, a small molecule that targets DDX3 has been synthesized by our laboratory, referred to as RK-33 [30]. RK-33 binds to the ATP-binding domain of DDX3 and inhibits its RNA-helicase activity [30]. Here, we show the growth inhibition of medulloblastoma cell lines by RK-33 which was associated with reduced transcript levels of WNT-regulated genes. We also demonstrate synergy between RK-33 treatment and radiation both *in vitro* and in a mouse model of medulloblastoma. Lastly, we also studied DDX3 expression in human medulloblastoma samples.

Materials and Methods

DAOY and UW228 cells were a kind gift from Dr. Michael Lim (Johns Hopkins University, Baltimore, MD, USA). The DAOY cell line (SHH subtype with a mutated p53 gene) was grown in DMEM/F-12 50/50, 1x (Dulbecco's Modification of Eagle's Medium/Ham's F-12 50/50 mix) with 10% fetal bovine serum, L-glutamine and 15 nM HEPES. The UW228 cell line (SHH subtype with a mutated p53 gene) was grown in MEM, 1x (Minimum Essential Medium Eagle) with Earle's salts and L-glutamine supplemented with 10% fetal bovine serum. The cell lines were maintained under sterile conditions in a humidified incubator with 5% CO_2 at 37°C. Transfection was performed using the JetPrime transfection reagent (Polyplus, New York, NY, USA) and TransLT1 (Mirus, Madison, WI, USA). For the DDX3 knockdown experiments, siControl (non-targeting pool) and siDDX3 sequences were purchased from Dharmacon, Lafayette, CO, USA.

Patient Samples

A medulloblastoma tissue microarray with 80 cases was previously assembled at the Johns Hopkins Hospital Department of Pathology. Survival data are available for these de-identified patient specimens under IRB approved protocol, NA_00015113. These cases were previously assigned to a molecular subgroup by the German Cancer Research Center (DKFZ), Heidelberg, Germany, using an immunohistochemical panel to identify 4 distinct subgroups; WNT, SHH, Group 3, and Group 4 using antibodies as previously described [16,33]. Missing cases were attributable to damaged or detached cores during cutting or staining, or to cores not containing tumor. Pathology was reviewed according to the 2007 WHO classification for central nervous system tumors [3]. Clinicopathological data were retrieved from the pathology report and patient files.

Immunohistochemistry

Four μm-thick sections were cut, mounted on Super Frost slides (Menzel & Glaeser, Brunswick, Germany), deparaffinized in xylene, and rehydrated in decreasing ethanol dilutions. Endogenous peroxidase activity was blocked with 1.5% hydrogen peroxide buffer for 15 minutes and was followed by antigen retrieval through boiling for 20 minutes in 10 mM citrate buffer (pH 6.0) for DDX3. Slides were subsequently incubated in a humidified chamber for 1 hour with anti-DDX3 (1:1000, pAb r647) [34]. After washing with PBS, slides were incubated with poly-HRP-anti-mouse/rabbit/rat IgG (BrightVision Immunologic, Duiven, The Netherlands) as a secondary antibody for 30 minutes at room temperature. Peroxidase activity was developed with diaminobenzidine and hydrogen peroxide substrate solution for 10 minutes. The slides were lightly counterstained with hematoxylin and mounted. Appropriate positive and negative controls were used throughout. Scoring of DDX3 was performed by P.V.D. The intensity of cytoplasmic DDX3 expression was scored semi-quantitatively as absent (0), low (1), moderate (2), or strong (3). Cases with a score of 0 to 1 were classified as having low DDX3 expression and evaluated against cases with strong expression.

Immunoblotting

DAOY and UW228 cells were harvested at 60–70% confluence for protein expression analysis. Standard SDS-PAGE and immunoblotting protocols were followed. The primary antibody used for DDX3 and actin was mouse monoclonal antibody and the secondary antibody used was anti-mouse antibody for both DDX3 and actin.

DDX3 Knockdown in Medulloblastoma Cell Lines

DAOY and UW228 cells were plated at 7.5×10^4 cells per well in six-well plates and incubated overnight. Cells were transfected with siDDX3 (25 nM) using the JetPrime transfection reagent. Media was refreshed 24 h after transfection. The cells were harvested after 72 h of transfection and protein concentration was estimated before Western blotting.

Cytotoxicity Assay

Cytotoxicity was determined using an MTS assay. DAOY and UW228 cells were plated in duplicates at 1×10^3 cells per well in a 96-well plate. After overnight incubation, cells were treated with

various concentrations of RK-33 (1 μM - 16 μM) and DMSO as a control, for about 72 h. An MTS reagent (10%) was added and cells incubated for an additional 2 h followed by reading absorbance at 490 nm (Victor V3, Perkin-Elmer).

Immunoblotting

DAOY and UW228 cells were plated at 1.5 x 10^5 cells per well in a six-well plate and incubated overnight. DAOY cells were treated with DMSO or 2.5 μM RK-33, while UW228 cells were treated with 3.5 μM RK-33. After 48 h, cells were lysed in SDS-extraction buffer (100 nM Tris–HCl, 2% SDS, 12% glycerol, 10 mM EDTA, pH 6.7) with an added protease inhibitor. Protein concentration was determined and 30 μg of each sample was loaded onto a 10% SDS-PAGE gel. After protein transfer to the PVDF membrane, DDX3 (1:500 in 5% BSA, mAb AO196) and actin (1:10,000 in 5% milk, A5441, Sigma-Aldrich, St. Louis, MO, USA) primary antibodies were added. After overnight incubation at 4°C, mouse secondary antibodies were added. The blots were developed with Clarity Western ECL (BioRad, Hercules, CA, USA) and imaged with a G-Box Chemi XR5 (Syngene, Frederick, MD, USA).

Cell Cycle Analysis

DAOY and UW228 cells were plated in duplicates at 1.5 x 10^5 cells per well in a six-well plate. After overnight incubation, cells were treated with RK-33 (1 μM and 2 μM) or DMSO. Briefly, after 24 h of RK-33 treatment, cells were trypsinized and fixed in 70% ethanol overnight at −20°C. Fixed cells were washed with PBS and resuspended in a DNA staining solution (5 μg/ml propidium iodide, 0.5 mg/ml RNase A) for one hour at room temperature. Cell cycle acquisition was performed on a FACScan I or FACScalibur instrument (BD Biosciences, San Jose, CA, USA). Debris was gated out and 10–25,000 cells were acquired per sample. Data were analyzed using FlowJo software (Tree Star Inc., Ashland, OR, USA).

Apoptosis Assay

DAOY and UW228 cells were plated in duplicates at 1.5 x 10^5 cells per well in six-well plates. After overnight incubation, cells were treated with RK-33 (2 μM) and DMSO as a control. After 24 h of drug treatment, apoptosis was measured with an Annexin V binding detection kit. Briefly, cells floating in the supernatant, along with the adherent fraction, were trypsinized and then washed. Cells were incubated with Annexin V-FITC and PI for 15 min at room temperature in the dark. Cells were immediately analyzed by flow cytometry. Debris was gated out while all other cells were studied. Viable cells excluded both Annexin V-FITC and PI. Early apoptotic cells were Annexin V-FITC-positive and PI-negative, whereas cells that were no longer viable, due to apoptotic or necrotic cell death, were positively stained by both Annexin V and PI. The amounts of stained cells in each quadrant was reported.

TCF Reporter Assays

The transcriptional activity of TCF4 was measured for DAOY and UW228 cells using the dual luciferase assay (Promega, Madison, WI, USA) according to the manufacturer's instructions. Briefly, DAOY and UW228 cells were plated at 3 x 10^4 cells per well in a 24-well plate. After overnight incubation, cells were transfected with 500 ng TOP-FLASH or FOP-FLASH constructs and 50 ng phRL Renilla constructs as a transfection control, using an LT1 transfection reagent. After overnight incubation, cells were treated with DMSO or 2.5 μM RK-33 for DAOY cells and 3.5 μM for UW228 cells and incubated for 24 h. The cells were lysed and the transcriptional activity of TCF4 was measured using a dual luciferase assay. For the DDX3 knockdown experiments, DAOY and UW228 cells were plated at 3 x 10^4 cells per well in a 24-well plate. After overnight incubation, cells were transfected with 10 nM siDDX3 for DAOY cells and 25 nM siDDX3 for UW228 cells using the JetPrime transfection reagent. The following morning, cells were transfected with TOP-FLASH and FOP-FLASH constructs using the TransLT1 transfection reagent and incubated for another 48 h, after which the cells were lysed for the luciferase assay. Luminescence was measured using a luminometer (Berthold Sirius, Oak Ridge, TN, USA). Relative TCF4-promoter activity was calculated by normalizing TOP-FLASH and FOP-FLASH readings for Renilla luciferase readings, and then, dividing normalized TOP-FLASH readings by normalized FOP-FLASH readings.

Quantitative Reverse Transcriptase Polymerase Chain Reaction

DAOY and UW228 cell lines were treated with RK-33 (2.5 μM and 3.5 μM) and siDDX3 (25 nM). After 24–48 h of treatment, cells were harvested and RNA was extracted using the RNeasy kit (Qiagen, Valencia, CA, USA), and cDNA was synthesized using the iScript cDNA synthesis kit (Bio-Rad, Hercules, CA, USA), followed by qPCR using SYBR green (Bio-Rad, Hercules, CA, USA) on a CFX96 Real-Time PCR detection system (Bio-Rad, Hercules, CA, USA). Amplification of 36B4, a housekeeping gene, was used to normalize gene expression values. Primer sequences: DDX3F: 5′-GGAGGAAGTACAGCCAG CAAAG-3′, DDX3R: 5′-CTGCCAATGCCATCGTAATCACTC-3′, AXIN2 F: 5‘-TCAAGTGCAAACTTTCGCCA-ACC-3′, AXIN2 R: 5′-TAGCCAGAACCTATGTGATAAGG-3′, MYC F: 5′-CGTCTCCAC-ACATCAGCACAA-3′, MYC R: 5′-CACTGTCC AACTTGACCCTCTTG-3′, CCND1 F: 5′-GGCGGAGGAGAA CAAACAGA-3′, CCND1 R: 5′-TGGCACAGAGGGCAACGA-3′, Survivin F: 5′-CCACCGCATCTCTACATTCA-3′, Survivin R: 5′-TATGTTCCTCTATGGG-GTCG-3′. Fold changes in mRNA expression were calculated using the $2^{(-\Delta\Delta CT)}$ method [35]. Statistical significance was calculated by performing a paired Student's t-test on the ΔCT values.

Clonogenic Assay

The radio-sensitivity of RK-33 was determined by a clonogenic survival assay. DAOY and UW228 cells at 200–700 were plated in duplicate in six-well plates and incubated overnight. The following day, cells were treated with RK-33 (1–3 μM) or DMSO. After 2.5 h of RK-33 treatment, the cells were exposed to increasing doses of radiation (0, 1, 2, and 3 Gy). After seven days of incubation, colonies consisting of more than 50 cells were scored. Colonies were washed with PBS and stained with 0.05% (w/v) crystal violet dye and then counted. The plating efficiency (PE) was calculated as “mean colony counts/cells seeded,” and the surviving fraction (SF) was calculated as “colonies / (cells seeded x plating efficiency),” and plating efficiency was defined as “mean colony counts for un-irradiated controls / cells seeded.”

In Vivo Combination of RK-33 Treatment With Radiation in Nude Mice

All mice were maintained under sterile conditions, and experiments were conducted according to the guidelines of the Johns Hopkins Animal Care and Use Committee. All animals were maintained under regulated temperature and humidity. Nude mice were injected in the flank with 1 x 10^6 DAOY cells mixed with matrigel. Mice were monitored until the tumor was felt by palpation.

Mice were distributed randomly over four groups of three mice: DMSO as a control; RK-33 (50 mg/kg); radiation (5 Gy); and a combination of RK-33 (50 mg/kg) and radiation (5 Gy). Mice were treated intraperitoneally with RK-33 every alternate day for two weeks. A single dose of radiation (5 Gy) was given using a Small Animal Radiation Research Platform (SARRP) with a circular beam focused on the tumor site. Mice were monitored for tumor growth. The size of tumors was measured over a period of time (42 days) and tumor volume was calculated [V = 1/2(length x width^2)] using Vernier calipers.

Statistical Analysis

The Cox proportional hazards analysis and Kaplan–Meier survival plots were used to evaluate differences in time to death between high and low values of DDX3 for subgroups of patient characteristics that had an adequate count of patients. The hazard ratio, 95% confidence interval and p-value for subgroups with adequate patients are provided. For subgroups where there were zero deaths for either the high or low value of DDX3 (perfect prediction) were not able to be evaluated for a hazard ratio.

All bars indicate standard deviation, except where indicated. Unpaired T-tests were used to determine significance. All experiments were performed at least twice (biological replicates) independently in replicates of 2 or 3. Graphs represent mean ± SD, $^*P < .05$, $^{**}P < .01$, $^{***}P < .001$.

Results

DDX3 Expression Increased in Medulloblastomas

To determine the expression levels of DDX3 in medulloblastoma samples, we evaluated a cohort of 80 medulloblastoma patients (15 samples were not scorable) for DDX3 expression by means of tissue microarrays. In normal brain tissue, we saw little or no expression of DDX3 (data not shown). However, in 31 of 56 (55%) pediatric medulloblastoma samples and in 6 of 9 (67%) adult medulloblastoma samples, we detected DDX3 expression Figure 1*A*. In addition, high cytoplasmic DDX3 expression was observed among different histological subtypes of medulloblastoma patients Figure 1, *A* and *B*. Importantly, no significant association between high and low cytoplasmic DDX3 and survival was observed in medulloblastoma patients Figure 1*C* and Table 1.

Table 1. Clinical Parameters

	Total	DDX3		HR	95% C.I.	*P* Value
		Low (Alive/Dead)	High (Alive/Dead)			
Age						
0–18	49	24 (14/10)	25 (14/11)	1.09	0.46–2.56	0.85
19+	8	3 (2/1)	5 (4/1)	0.45	0.03–7.37	0.57
Gender						
Female	25	14 (7/7)	11 (8/3)	0.40	0.10–1.56	0.19
Male	34	13 (9/4)	21 (10/11)	1.98	0.63–6.23	0.24
Race						
White	30	15 (7/8)	15 (9/6)	0.77	0.27–2.22	0.63
Black	11	6 (4/2)	5 (3/2)	1.11	0.15–8.16	0.92
German subgroup						
C	7	3 (0/3)	4 (0/4)	0.58	0.10–3.49	0.55
D	12	4 (3/1)	8 (6/2)	0.70	0.06–7.92	0.78
SHH	23	9 (9/0)	14 (10/4)	NA	NA	NA
Subtype						
Classic	26	11 (8/3)	15 (8/7)	1.78	0.46–6.88	0.41
Mod A	8	4 (3/1)	4 (3/1)	1.41	0.09–22.64	0.81
Nodular	10	4 (4/0)	6 (5/1)	NA	NA	NA
Sev A	6	2 (0/2)	4 (1/3)	0.16	0.01–1.75	0.13

Correlations between DDX3 and other clinicopathological variables in pediatric medulloblastoma patients. *P* values calculated by Cox proportional hazard analysis. HR, Hazard Ratio; C.I., Confidence Interval.

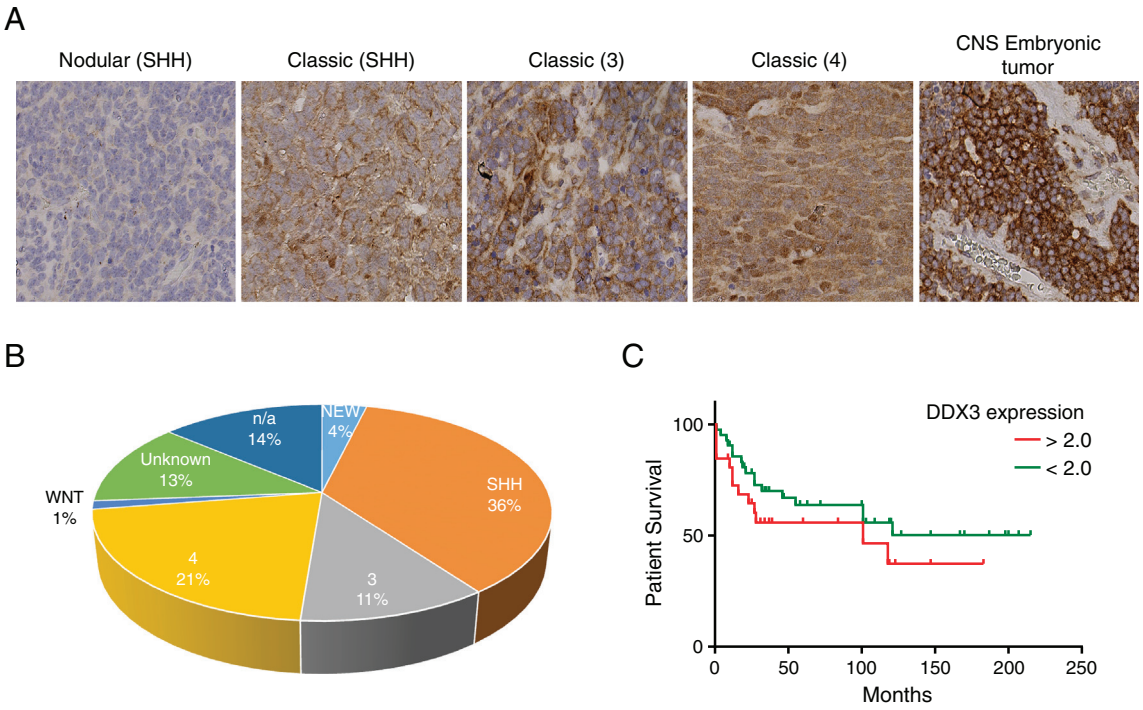

Figure 1. DDX3 expression in patients with medulloblastoma. A. DDX3 expression in the different molecular subgroup of pediatric and adult medulloblastoma as seen by immunohistochemical staining B. Sample distribution of the different molecular subgroups of medulloblastoma (n = 65) used in our study. C. Kaplan–Meier curve showing overall survival of medulloblastoma patients with low (<2) and high (>2) DDX3 expressing tumors.

Inhibition of DDX3 in Medulloblastoma Cell Lines Decreased Proliferation

To ascertain whether DDX3 inhibition decreases proliferation, we initially assessed DDX3 expression levels in the medulloblastoma cell lines DAOY and UW228. As shown in Figure 2*A*, both these cell lines express high levels of DDX3. To determine the role of DDX3 on the growth of DAOY and UW228 cells, we specifically knocked down DDX3 expression using a validated siRNA [31] Figure 2*B*. As shown in Figure 2*C*, the knockdown of DDX3 resulted in reduced cellular proliferation.

RK-33 Inhibited Cell Viability in Medulloblastoma Cell Lines

As DDX3 expression is high in medulloblastoma cell lines, we next evaluated whether these cell lines were sensitive to RK-33, a small molecule that targets DDX3. The structure of RK-33 is shown in Supplementary Figure 1. DAOY and UW228 cell lines were treated with various concentrations of RK-33, and cell viability was measured on day 3 with an MTS assay. Both the DAOY and the UW228 cell lines were sensitive to RK-33, with IC_{50} values of 2.5 μM and 3.5 μM, respectively Figure 3*A*. In order to determine the effect of RK-33 on DDX3 expression levels, we treated DAOY and UW228 cell lines with IC_{50} values of RK-33. After 24 h of treatment with RK-33, we scored for DDX3 expression levels by western blotting. The result showed decreased levels of DDX3 expression in both the DAOY and the UW228 cell lines, as shown in Figure 3*B*. Photomicrographs of cells treated with RK-33 or DMSO are shown in Figure 3*C*. Based on these observations, we can conclude that RK-33 can effectively reduce DDX3 levels, as a result of which cell death mechanisms are potentially enhanced.

To extend the findings, we evaluated the expression level of DDX3 in two additional medulloblastoma cell lines: D425-Med and HD-MB03 cells. As shown in Supplementary Figure 2, both of these cell lines express DDX3 with D425-Med cells exhibiting somewhat higher levels then HD-MB03 cells. Furthermore, both D425-Med and HD-MB03 cells were sensitive to RK-33 treatment when grown as monolayers on adherent plates with IC_{50} values of 2.3 and 6.5 μM respectively Supplementary Figure 2*A*. Moreover, as shown in the Calcein AM green fluorescence (viable cells) photomicrographs and plots of Supplementary Figure 2, *B* and *C*. when these cell lines were grown in suspension in non-adherent plates their sensitivity to RK-33 treatment remained in a similar range of IC_{50} values of 4.5 and 5.8 μM for D425-Med and HD-MB03 cells respectively.

RK-33 Induced a G1-Phase Cell Cycle Arrest and Caused Apoptosis

Next, to define the effects of RK-33 on cell cycle profile, we performed flow cytometry analysis on RK-33-treated DAOY and UW228 cells. Both DAOY and UW228 cells exhibited G1 arrest within 24 h of RK-33 treatment Figure 3*D*. This is indicative that RK-33-induced G1 arrest in both DAOY and UW228 cells might be dependent on DDX3 levels in these two cell lines.

In order to delineate whether the cell cycle arrest at the G1 phase as a result of RK-33 treatment was due to apoptosis, we next performed flow cytometric analysis using Annexin V/PI staining. DAOY and UW228 cells were treated with RK-33 (2 μM), incubated for 24 h, and subjected to Annexin V/PI staining to assess the percentage of viable, early apoptotic, and late apoptotic cells Figure 4*A*. The analysis showed that the number of viable cells, pre-apoptotic, and apoptotic cells in DAOY was 83%, 3%, and 3%, respectively. In UW228, the number of viable cells, pre-apoptotic, and apoptotic cells was 74%, 4%, and 6%, respectively Figure 4*B*. From this observation, we conclude that treatment of DAOY and UW228 cells with RK-33 induced a G1-phase cell cycle arrest with minor cell death.

DDX3 Knockdown and RK-33 Treatment Decreased WNT/β-Catenin Signaling

In order to investigate the relation between the interference of the oncogenic WNT/β-catenin pathway with the observed reduction in proliferation, we tested whether DDX3 inhibition causes a reduction in TCF promoter activity using a TOP/FOP luciferase assay. By transfecting DDX3 knockdown cell lines using TOP-FLASH or FOP-FLASH, the knockdown of DDX3 resulted in a significant

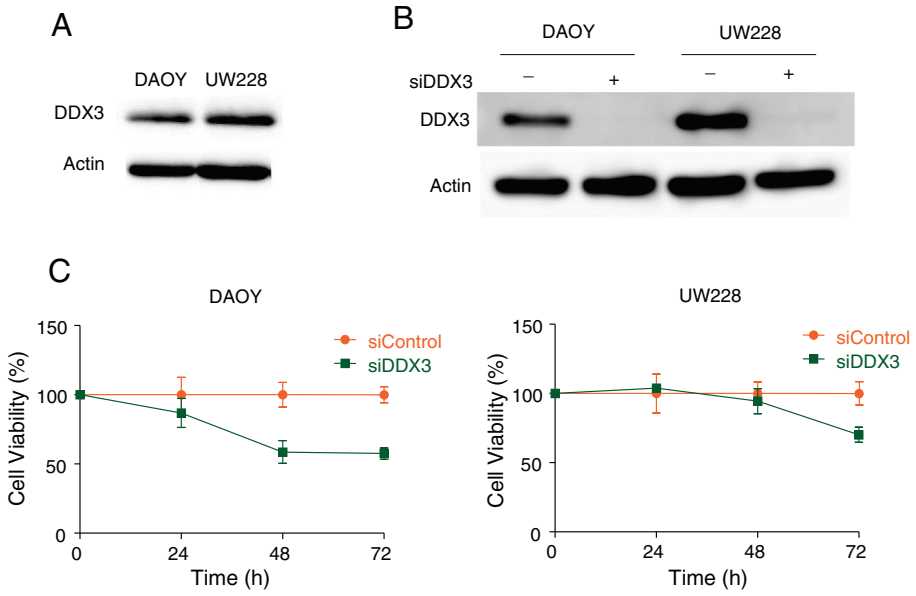

Figure 2. Inhibition of DDX3 in medulloblastoma cell lines results in a decrease of proliferation. A. Intrinsic DDX3 expression levels in DAOY and UW228 cells, as detected by immunoblotting B. Immunoblotting showing DDX3 expression levels after knockdown of DDX3 using 25 nM siDDX3. C. Proliferation assay of DAOY and UW228 cells after knockdown of DDX3 measured by MTS assay.

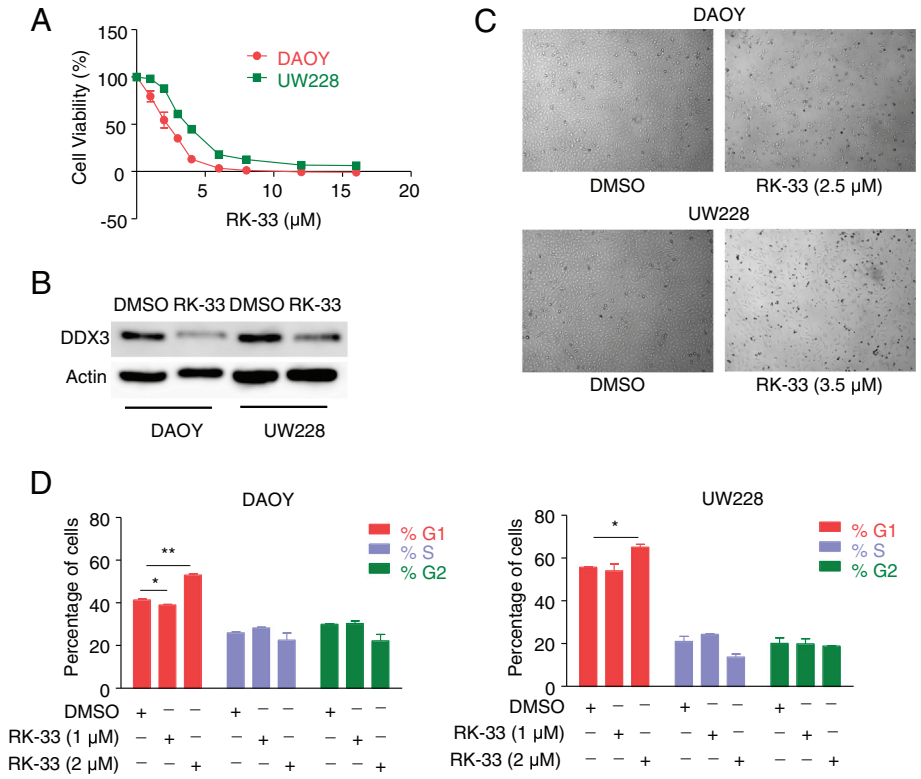

Figure 3. RK-33 inhibits cell viability in medulloblastoma cell lines. A. Cytotoxicity assay showing the sensitivity of DAOY and UW228 cells to various concentrations of RK-33 after 72 h incubation as measured by MTS assay. B. Immunoblots showing DDX3 expression levels in medulloblastoma cell lines after treatment with RK-33 for 48 h. C. Cells treated with RK-33 indicating cell death. D. Graph displaying changes in cell cycle phases after treating DAOY and UW228 cells with RK-33 for 24 h.

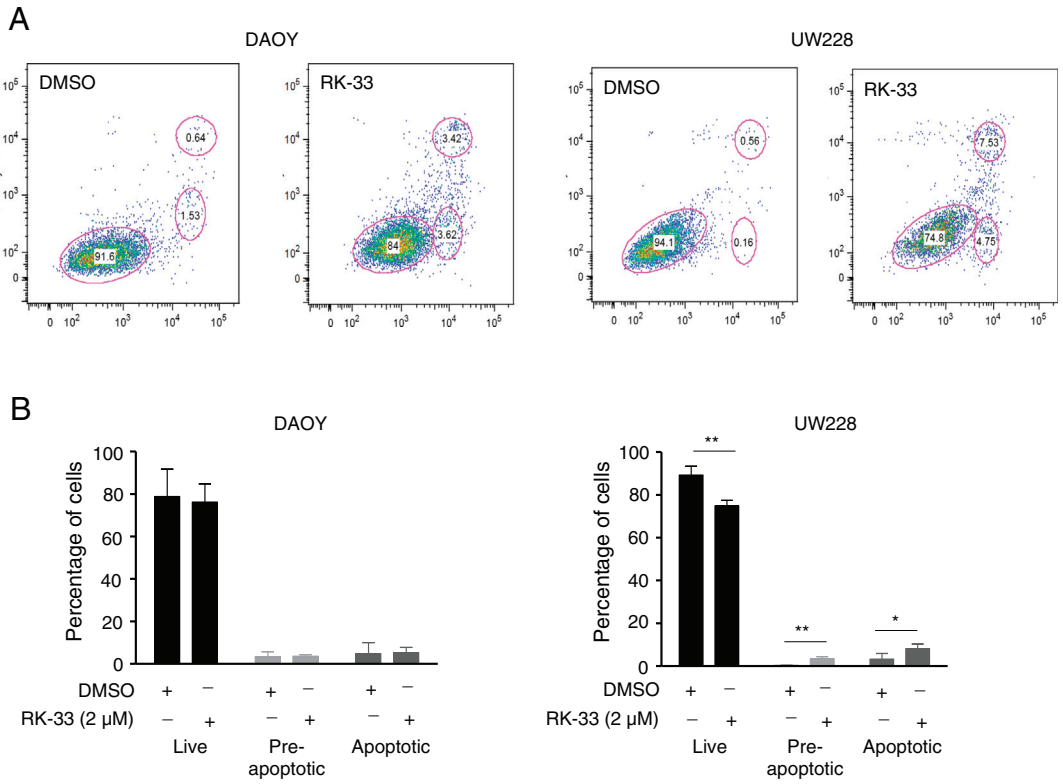

Figure 4. Induction of apoptosis in DAOY and UW228 cells treated with RK-33. A. Representative histograms displaying the flow cytometric density plot of Annexin V/PI staining after DAOY and UW228 cell line treatment with RK-33 (2 μM) or DMSO (control) for 24 h. B. Histogram representing the average population of viable cells, pre-apoptotic, and apoptotic cells that were determined by estimating the stained cells with Annexin V/PI staining.

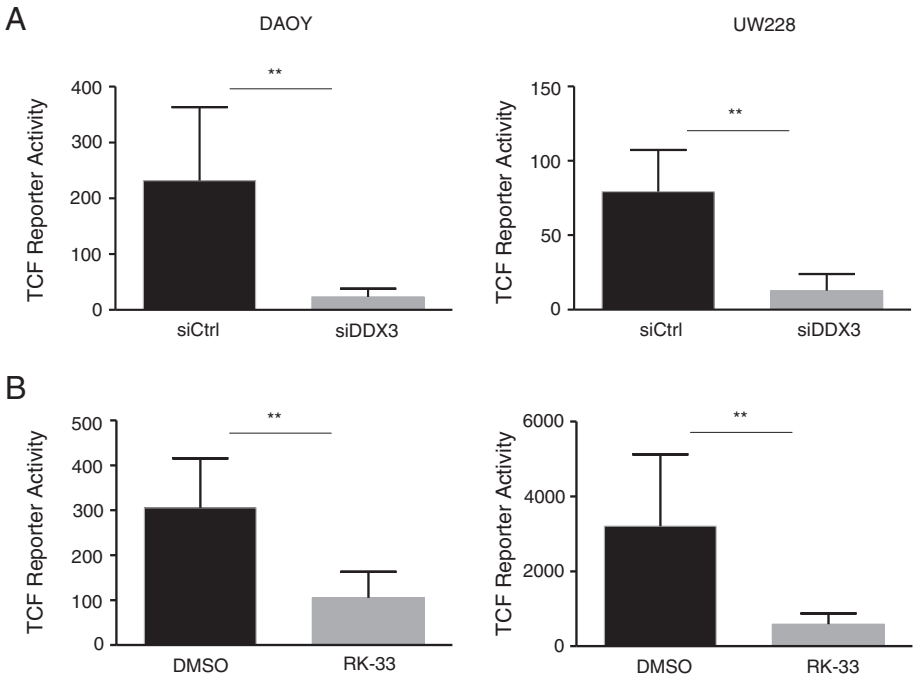

Figure 5. WNT signaling activity is reduced by DDX3 inhibition in DAOY and UW228 cells. A. Histogram displaying TCF reporter activity of cell lines after treatment with 10 nM siDDX3 for DAOY cells and 25 nM for UW228 cells. B. TCF reporter activities after treatment with RK-33 (2.5 μM for DAOY cells and 3.5 μM for UW228 cells).

decrease in TCF activity in both DAOY and UW228 cells. Similarly, RK-33 also significantly reduced TCF activity in both DAOY and UW228 cells Figure 5, *A* and *B*.

Since the WNT/β-catenin signaling pathway activates downstream target genes, such as Axin2, CCND1, MYC, and Survivin, which promote tumor progression, we next evaluated whether reduced TCF reporter activity in medulloblastoma cell lines also resulted in reduced expression of mRNA of TCF regulated genes. From this analysis, we observed that DDX3 knockdown resulted in a reduced expression of Axin2, CCND1, MYC, and Survivin in both DAOY and UW228 cell lines. RK-33 treatment also significantly reduced transcription of Axin2, CCND1, MYC, and Survivin, as shown in Figure 6. Based on these findings, we conclude that DDX3 inhibition resulted in decreased WNT/β-catenin signaling in both DAOY and UW228 cells, which further confirms the role of DDX3 in cell cycle progression and in the generation of a tumor phenotype.

Combination of RK-33 and Radiation Exhibited Synergistic Cell Death Effect, Both In Vitro and in a Preclinical Model of Medulloblastoma

In order to evaluate the effect of RK-33 in combination with radiation, we treated DAOY and UW228 cell lines with RK-33 and different doses of radiation in a colony forming assay. Based on the data obtained, we observed that a combination of RK-33 and radiation resulted in a significantly higher inhibitory effect than using single treatment of either RK-33 or radiation Figure 7*A*. This indicates that RK-33 is able to radiosensitize DAOY and the UW228 cell lines, resulting in enhanced cell death.

To determine whether RK-33 could be used clinically as a radiosensitizer for medulloblastoma treatment, we treated tumors generated using DAOY cell line in nude mice, with RK-33 in combination with radiation. Following tumor generation in the flank, mice were randomly grouped and were treated with DMSO, RK-33, radiation (5 Gy), and a combination of RK-33 and radiation (5 Gy). Of the three different treatment groups, 5 Gy in combination with RK-33 demonstrated the highest tumor reduction Figure 7*B*. This is indicative of the use of RK-33 as a potential radiosensitizer for the treatment of medulloblastoma.

Discussion

About 10% of medulloblastomas are driven by mutations in the WNT signaling pathway, but are considered a low risk subgroup [36]. This subgroup is identified by the β-catenin nucleo-positive immunophenotype and is associated with a significantly better overall survival, thus suggesting that nuclear β-catenin accumulation is a marker of favorable outcome in medulloblastoma [37]. In a normal cell, the cytoplasmic β-catenin levels are maintained by the phosphorylation of β-catenin by a cytoplasmic destruction complex consisting of APC, axin, casein kinase 1α (CK1α), and glycogen synthase kinase (GSK3β), and further β-catenin is degraded by the ubiquitin proteasome complex [38,39]. Mutations in the phosphorylation site lead to β-catenin stabilization, which is translocated to the nucleus where it interacts with the TCF/LEF complex and causes up-regulation of WNT target genes, such as Axin2, CCND1, MYC, and Survivin [8,40–43].

Earlier reports have shown that DDX3 is among the most mutated gene in pediatric and adult medulloblastoma [26,44]. A positive correlation between the high expression of DDX3 and poor prognosis has been reported in human tumors [45]. DDX3 mutations often occur simultaneously along with β-catenin mutations, and this mutant DDX3 increases the activity of mutated β-catenin activity, thereby enhancing the nuclear translocation of β-catenin. The role of DDX3 in WNT/β-catenin signaling was first reported by Cruciat et al. [46]. Since a percentage of medulloblastomas are driven by mutations in the WNT signaling pathway, we investigated the possible role of DDX3 in WNT-associated medulloblastoma. Furthermore, we investigated the

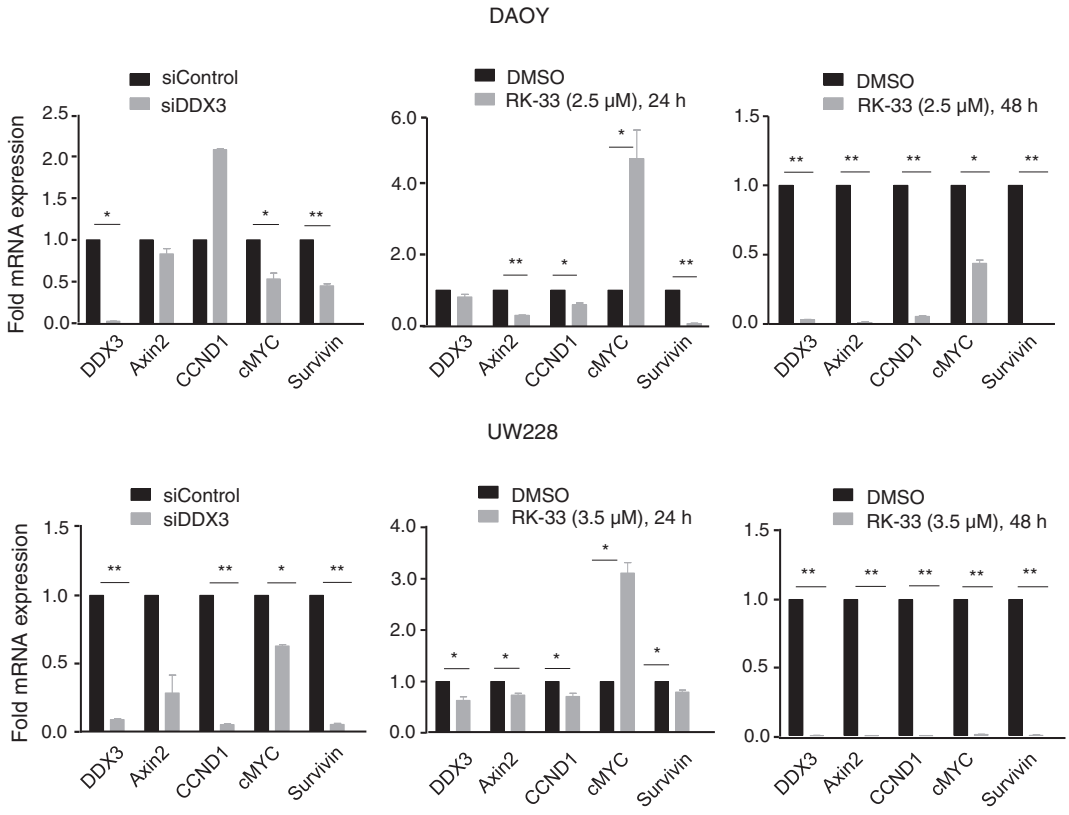

Figure 6. Quantitative reverse transcriptase polymerase chain reaction. Relative mRNA expression of WNT target genes after knockdown of DDX3 with 25 nM siDDX3 in DAOY and UW228 cell lines and RK-33 treatment (2.5 μM for DAOY cells and 3.5 μM for UW228 cells) for 24–48 h.

potent anti-tumor activity of RK-33, a small molecule inhibitor of DDX3, on medulloblastoma cell lines *in vitro* and *in vivo*. We demonstrated that DDX3 is over-expressed in medulloblastoma cell lines, and targeting DDX3 with RK-33 not only reduced WNT signaling, but also caused a G1 arrest. We also showed that the inhibition of DDX3 resulted in reduced proliferation of medulloblastoma cell lines.

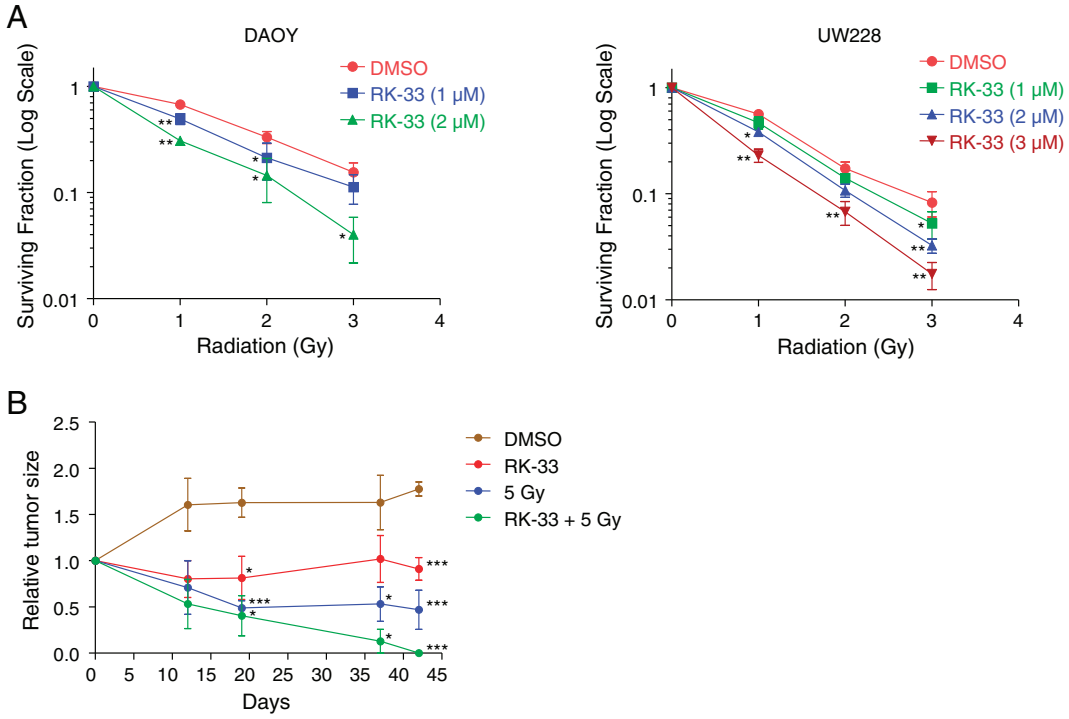

Figure 7. *In vitro* and *in vivo* combination of RK-33 and radiation. A. Effect of a combination of RK-33 of various concentrations (1–3 μM) and radiation of different doses (0 Gy to 3 Gy) on the survival of DAOY and UW228 cell lines. B. Graph detailing tumor size effects in DAOY-inoculated SCID mice after treatment with DMSO, RK-33, radiation (5 Gy), and a combination of RK-33 and radiation. Bars indicate SEM.

This demonstrates the dependence of medulloblastoma cell lines on DDX3 for their survival. However, some reports have shown a contradictory role for DDX3 as both an oncogene [28,30,47] as well as tumor suppressor gene [48,49]. Several known WNT/β-catenin downstream targets, such as Axin2, CCND1, MYC, and Survivin, were decreased by RK-33 treatment, as demonstrated by RT-PCR analysis in the medulloblastoma cell lines used in this study. Earlier, it was shown that Norcantharidin impairs medulloblastoma growth by inhibiting WNT/β-catenin signaling [50]. The biflavone ginkgetin also suppresses the growth of medulloblastoma by inhibiting the WNT/β-catenin signaling pathway, inducing G2/M phase arrest, and also reducing the expression of the downstream target genes of the WNT/β-catenin signaling pathway, such as Axin2, CCNDI, and Survivin in DAOY cells [51]. Our results also parallel those, which were reported earlier.

The *in vivo* non-toxic effect, as well as radio-sensitization of RK-33, has been reported previously in lung cancer and prostate cancer from our laboratory [30,32]. Based on these previous results, we evaluated the effect of RK-33 as a radio-sensitizer by performing *in vitro* clonogenic assays using DAOY and UW228 cells. A combination of 2 μM RK-33 and 3 Gy radiation in the DAOY cell line, and a combination of 3 μM RK-33 and 3 Gy radiation in UW228 cell line, reduced the clonogenic ability compared to RK-33 or radiation alone. Treatment of mice with DAOY flank tumors with a combination of RK-33 and a 5 Gy radiation dose showed a significant reduction in tumor size compared to RK-33 and radiation alone. Moreover, in both pediatric and adult patient medulloblastoma samples, we detected that over 55% and 66% of the samples had DDX3 expression, respectively.

Conclusions

Currently, in the field of medulloblastoma, extensive attention has been focused on the post-therapy quality of life and reducing the risk of long-term side effects. The goal is to minimize the intensity of the treatment, as well as use less toxic - and more targeted - novel agents in the treatment of medulloblastoma. In this regard, RK-33, a small molecule inhibitor of DDX3, acts as a promising novel therapeutic agent that not only can reduce the toxicities associated with the treatment, but also reduce the dose of radiation in the treatment of medulloblastoma. In conclusion, RK-33 acts as a promising small molecule inhibitor that can target and induce cell death in medulloblastomas in which DDX3/WNT-β-catenin is over-expressed.

Funding

Funding for this work was supported by Safeway (VR) and FAMRI (VR).

Acknowledgments

We would like to acknowledge support for the statistical analysis from Carol Thompson of the National Center for Research Resources and the National Center for Advancing Translational Sciences (NCATS) of the National Institutes of Health through Grant Number 1UL1TR001079.

Appendix A. Supplementary Data

Supplementary data to this article can be found online at https://doi.org/10.1016/j.tranon.2018.09.002.

References

[1] Rogers HA, Sousa S, Salto C, Arenas E, Coyle B, and Grundy RG (2012). WNT/beta-catenin pathway activation in Myc immortalised cerebellar progenitor cells inhibits neuronal differentiation and generates tumours resembling medulloblastoma. *Br J Cancer* **107**, 1144–1152.

[2] Jones DT, Jager N, Kool M, Zichner T, Hutter B, Sultan M, Cho YJ, Pugh TJ, Hovestadt V, and Stutz AM, et al (2012). Dissecting the genomic complexity underlying medulloblastoma. *Nature* **488**, 100–105.

[3] Louis DN, Ohgaki H, Wiestler OD, Cavenee WK, Burger PC, Jouvet A, Scheithauer BW, and Kleihues P (2007). The 2007 WHO classification of tumours of the central nervous system. *Acta Neuropathol* **114**, 97–109.

[4] Gilbertson RJ and Ellison DW (2008). The origins of medulloblastoma subtypes. *Annu Rev Pathol* **3**, 341–365.

[5] Schwalbe EC, Lindsey JC, Nakjang S, Crosier S, Smith AJ, Hicks D, Rafiee G, Hill RM, Iliasova A, and Stone T, et al (2017). Novel molecular subgroups for clinical classification and outcome prediction in childhood medulloblastoma: a cohort study. *Lancet Oncol* **18**, 958–971.

[6] Northcott PA, Buchhalter I, Morrissy AS, Hovestadt V, Weischenfeldt J, Ehrenberger T, Grobner S, Segura-Wang M, Zichner T, and Rudneva VA, et al (2017). The whole-genome landscape of medulloblastoma subtypes. *Nature* **547**, 311–317.

[7] Ellison DW, Kocak M, Dalton J, Megahed H, Lusher ME, Ryan SL, Zhao W, Nicholson SL, Taylor RE, and Bailey S, et al (2011). Definition of disease-risk stratification groups in childhood medulloblastoma using combined clinical, pathologic, and molecular variables. *J Clin Oncol* **29**, 1400–1407.

[8] Zurawel RH, Chiappa SA, Allen C, and Raffel C (1998). Sporadic medulloblastomas contain oncogenic beta-catenin mutations. *Cancer Res* **58**, 896–899.

[9] Ellison DW, Dalton J, Kocak M, Nicholson SL, Fraga C, Neale G, Kenney AM, Brat DJ, Perry A, and Yong WH, et al (2011). Medulloblastoma: clinicopathological correlates of SHH, WNT, and non-SHH/WNT molecular subgroups. *Acta Neuropathol* **121**, 381–396.

[10] Gibson P, Tong Y, Robinson G, Thompson MC, Currle DS, Eden C, Kranenburg TA, Hogg T, Poppleton H, and Martin J, et al (2010). Subtypes of medulloblastoma have distinct developmental origins. *Nature* **468**, 1095–1099.

[11] Kool M, Korshunov A, Remke M, Jones DT, Schlanstein M, Northcott PA, Cho YJ, Koster J, Schouten-van Meeteren A, and van Vuurden D, et al (2012). Molecular subgroups of medulloblastoma: an international meta-analysis of transcriptome, genetic aberrations, and clinical data of WNT, SHH, Group 3, and Group 4 medulloblastomas. *Acta Neuropathol* **123**, 473–484.

[12] Yauch RL, Dijkgraaf GJ, Alicke B, Januario T, Ahn CP, Holcomb T, Pujara K, Stinson J, Callahan CA, and Tang T, et al (2009). Smoothened mutation confers resistance to a Hedgehog pathway inhibitor in medulloblastoma. *Science* **326**, 572–574.

[13] Northcott PA, Hielscher T, Dubuc A, Mack S, Shih D, Remke M, Al-Halabi H, Albrecht S, Jabado N, and Eberhart CG, et al (2011). Pediatric and adult sonic hedgehog medulloblastomas are clinically and molecularly distinct. *Acta Neuropathol* **122**, 231–240.

[14] Slade I, Murray A, Hanks S, Kumar A, Walker L, Hargrave D, Douglas J, Stiller C, Izatt L, and Rahman N (2011). Heterogeneity of familial medulloblastoma and contribution of germline PTCH1 and SUFU mutations to sporadic medulloblastoma. *Fam Cancer* **10**, 337–342.

[15] Cho YJ, Tsherniak A, Tamayo P, Santagata S, Ligon A, Greulich H, Berhoukim R, Amani V, Goumnerova L, and Eberhart CG, et al (2011). Integrative genomic analysis of medulloblastoma identifies a molecular subgroup that drives poor clinical outcome. *J Clin Oncol* **29**, 1424–1430.

[16] Northcott PA, Korshunov A, Witt H, Hielscher T, Eberhart CG, Mack S, Bouffet E, Clifford SC, Hawkins CE, and French P, et al (2011). Medulloblastoma comprises four distinct molecular variants. *J Clin Oncol* **29**, 1408–1414.

[17] Soulat D, Burckstummer T, Westermayer S, Goncalves A, Bauch A, Stefanovic A, Hantschel O, Bennett KL, Decker T, and Superti-Furga G (2008). The DEAD-box helicase DDX3X is a critical component of the TANK-binding kinase 1-dependent innate immune response. *EMBO J* **27**, 2135–2146.

[18] Chuang RY, Weaver PL, Liu Z, and Chang TH (1997). Requirement of the DEAD-Box protein ded1p for messenger RNA translation. *Science* **275**, 1468–1471.

[19] Lee CS, Dias AP, Jedrychowski M, Patel AH, Hsu JL, and Reed R (2008). Human DDX3 functions in translation and interacts with the translation initiation factor eIF3. *Nucleic Acids Res* **36**, 4708–4718.

[20] Merz C, Urlaub H, Will CL, and Luhrmann R (2007). Protein composition of human mRNPs spliced in vitro and differential requirements for mRNP protein recruitment. *RNA* **13**, 116–128.

[21] Yedavalli VS, Neuveut C, Chi YH, Kleiman L, and Jeang KT (2004). Requirement of DDX3 DEAD box RNA helicase for HIV-1 Rev-RRE export function. *Cell* **119**, 381–392.

[22] Lai MC, Lee YH, and Tarn WY (2008). The DEAD-box RNA helicase DDX3 associates with export messenger ribonucleoproteins as well as tip-associated protein and participates in translational control. *Mol Biol Cell* **19**, 3847–3858.

[23] Wang L, Lawrence MS, Wan Y, Stojanov P, Sougnez C, Stevenson K, Werner L, Sivachenko A, DeLuca DS, and Zhang L, et al (2011). SF3B1 and other novel cancer genes in chronic lymphocytic leukemia. *N Engl J Med* **365**, 2497–2506.

[24] Stransky N, Egloff AM, Tward AD, Kostic AD, Cibulskis K, Sivachenko A, Kryukov GV, Lawrence MS, Sougnez C, and McKenna A, et al (2011). The mutational landscape of head and neck squamous cell carcinoma. *Science* **333**, 1157–1160.

[25] Brandimarte L, La Starza R, Gianfelici V, Barba G, Pierini V, Di Giacomo D, Cools J, Elia L, Vitale A, and Luciano L, et al (2014). DDX3X-MLLT10 fusion in adults with NOTCH1 positive T-cell acute lymphoblastic leukemia. *Haematologica* **99**, 64–66.

[26] Northcott PA, Jones DT, Kool M, Robinson GW, Gilbertson RJ, Cho YJ, Pomeroy SL, Korshunov A, Lichter P, and Taylor MD, et al (2012). Medulloblastomics: the end of the beginning. *Nat Rev Cancer* **12**, 818–834.

[27] Pugh TJ, Weeraratne SD, Archer TC, Pomeranz Krummel DA, Auclair D, Bochicchio J, Carneiro MO, Carter SL, Cibulskis K, and Erlich RL, et al (2012). Medulloblastoma exome sequencing uncovers subtype-specific somatic mutations. *Nature* **488**, 106–110.

[28] Chen HH, Yu HI, Cho WC, and Tarn WY (2015). DDX3 modulates cell adhesion and motility and cancer cell metastasis via Rac1-mediated signaling pathway. *Oncogene* **34**, 2790–2800.

[29] He TY, Wu DW, Lin PL, Wang L, Huang CC, Chou MC, and Lee H (2016). DDX3 promotes tumor invasion in colorectal cancer via the CK1epsilon/Dvl2 axis. *Sci Rep* **6**21483.

[30] Bol GM, Vesuna F, Xie M, Zeng J, Aziz K, Gandhi N, Levine A, Irving A, Korz D, and Tantravedi S, et al (2015). Targeting DDX3 with a small molecule inhibitor for lung cancer therapy. *EMBO Mol Med* **7**, 648–669.

[31] Heerma van Voss MR, Vesuna F, Trumpi K, Brilliant J, Berlinicke C, de Leng W, Kranenburg O, Offerhaus GJ, Burger H, and van der Wall E, et al (2015). Identification of the DEAD box RNA helicase DDX3 as a therapeutic target in colorectal cancer. *Oncotarget* **6**, 28312–28326.

[32] Xie M, Vesuna F, Tantravedi S, Bol GM, Heerma van Voss MR, Nugent K, Malek R, Gabrielson KL, Van Diest PJ, and Tran PT, et al (2016). RK-33 radiosensitizes prostate cancer cells by blocking the RNA helicase DDX3. *Cancer Res* **76**(21), 6340–6350.

[33] Remke M, Hielscher T, Korshunov A, Northcott PA, Bender S, Kool M, Westermann F, Benner A, Cin H, and Ryzhova M, et al (2011). FSTL5 is a marker of poor prognosis in non-WNT/non-SHH medulloblastoma. *J Clin Oncol* **29**, 3852–3861.

[34] Angus AG, Dalrymple D, Boulant S, McGivern DR, Clayton RF, Scott MJ, Adair R, Graham S, Owsianka AM, and Targett-Adams P, et al (2010). Requirement of cellular DDX3 for hepatitis C virus replication is unrelated to its interaction with the viral core protein. *J Gen Virol* **91**, 122–132.

[35] Yuan JS, Reed A, Chen F, and Stewart Jr CN (2006). Statistical analysis of real-time PCR data. *BMC Bioinformatics* **7**, 85–96.

[36] Clifford SC, Lusher ME, Lindsey JC, Langdon JA, Gilbertson RJ, Straughton D, and Ellison DW (2006). Wnt/Wingless pathway activation and chromosome 6 loss characterize a distinct molecular sub-group of medulloblastomas associated with a favorable prognosis. *Cell Cycle* **5**, 2666–2670.

[37] Ellison DW, Onilude OE, Lindsey JC, Lusher ME, Weston CL, Taylor RE, Pearson AD, Clifford SC, and United Kingdom Children's Cancer Study Group Brain Tumour C (2005). beta-Catenin status predicts a favorable outcome in childhood medulloblastoma: the United Kingdom Children's Cancer Study Group Brain Tumour Committee. *J Clin Oncol* **23**, 7951–7957.

[38] Kimelman D and Xu W (2006). beta-catenin destruction complex: insights and questions from a structural perspective. *Oncogene* **25**, 7482–7491.

[39] Liu C, Li Y, Semenov M, Han C, Baeg GH, Tan Y, Zhang Z, Lin X, and He X (2002). Control of beta-catenin phosphorylation/degradation by a dual-kinase mechanism. *Cell* **108**, 837–847.

[40] Koch A, Waha A, Tonn JC, Sorensen N, Berthold F, Wolter M, Reifenberger J, Hartmann W, Friedl W, and Reifenberger G, et al (2001). Somatic mutations of WNT/wingless signaling pathway components in primitive neuroectodermal tumors. *Int J Cancer* **93**, 445–449.

[41] Eberhart CG, Tihan T, and Burger PC (2000). Nuclear localization and mutation of beta-catenin in medulloblastomas. *J Neuropathol Exp Neurol* **59**, 333–337.

[42] Tetsu O and McCormick F (1999). Beta-catenin regulates expression of cyclin D1 in colon carcinoma cells. *Nature* **398**, 422–426.

[43] He TC, Sparks AB, Rago C, Hermeking H, Zawel L, da Costa LT, Morin PJ, Vogelstein B, and Kinzler KW (1998). Identification of c-MYC as a target of the APC pathway. *Science* **281**, 1509–1512.

[44] Kool M, Jones DT, Jager N, Northcott PA, Pugh TJ, Hovestadt V, Piro RM, Esparza LA, Markant SL, and Remke M, et al (2014). Genome sequencing of SHH medulloblastoma predicts genotype-related response to smoothened inhibition. *Cancer Cell* **25**, 393–405.

[45] Miao X, Yang ZL, Xiong L, Zou Q, Yuan Y, Li J, Liang L, Chen M, and Chen S (2013). Nectin-2 and DDX3 are biomarkers for metastasis and poor prognosis of squamous cell/adenosquamous carcinomas and adenocarcinoma of gallbladder. *Int J Clin Exp Pathol* **6**, 179–190.

[46] Cruciat CM, Dolde C, de Groot RE, Ohkawara B, Reinhard C, Korswagen HC, and Niehrs C (2013). RNA helicase DDX3 is a regulatory subunit of casein kinase 1 in Wnt-beta-catenin signaling. *Science* **339**, 1436–1441.

[47] Botlagunta M, Vesuna F, Mironchik Y, Raman A, Lisok A, Winnard Jr P, Mukadam S, Van Diest P, Chen JH, and Farabaugh P, et al (2008). Oncogenic role of DDX3 in breast cancer biogenesis. *Oncogene* **27**, 3912–3922.

[48] Chao CH, Chen CM, Cheng PL, Shih JW, Tsou AP, and Lee YH (2006). DDX3, a DEAD box RNA helicase with tumor growth-suppressive property and transcriptional regulation activity of the p21waf1/cip1 promoter, is a candidate tumor suppressor. *Cancer Res* **66**, 6579–6588.

[49] Wu DW, Lee MC, Wang J, Chen CY, Cheng YW, and Lee H (2014). DDX3 loss by p53 inactivation promotes tumor malignancy via the MDM2/Slug/E-cadherin pathway and poor patient outcome in non-small-cell lung cancer. *Oncogene* **33**, 1515–1526.

[50] Cimmino F, Scoppettuolo MN, Carotenuto M, De Antonellis P, Dato VD, De Vita G, and Zollo M (2012). Norcantharidin impairs medulloblastoma growth by inhibition of Wnt/beta-catenin signaling. *J Neurooncol* **106**, 59–70.

[51] Ye ZN, Yu MY, Kong LM, Wang WH, Yang YF, Liu JQ, Qiu MH, and Li Y (2015). Biflavone ginkgetin, a novel Wnt inhibitor, suppresses the growth of medulloblastoma. *Nat Prod Bioprospect* **5**(2), 91–97.